DOI: https://doi.org/10.3897/arphapreprints.e151900

Temporal Altitudinal Biogeographic Shifts (TABS): R package for reconstructing biogeographic shifts in terrestrial and marine habitats over time

Johannes De Groeve, Kenneth Rijsdijk, Eline Rentier, Suzette G.A. Flantua, Sietze Norder

Research Paper

Temporal Altitudinal Biogeographic Shifts (TABS): R package for reconstructing biogeographic shifts in terrestrial and marine habitats over time

Authors: Johannes De Groeve[1], Kenneth F. Rijsdijk[1], Eline S. Rentier[2], Suzette G.A. Flantua[2], Sietze J. Norder[3]

1. Institute for Biodiversity and Ecosystem Dynamics, University of Amsterdam, Amsterdam, Netherlands
2. Department of Biological Sciences and Bjerknes Centre for Climate Research, University of Bergen, Bergen, Norway
3. Copernicus Institute of Sustainable Development, Utrecht University, Utrecht, Netherlands

Corresponding author: Johannes De Groeve j.degroeve@uva.nl; degroevejohannes@gmail.com

JDG: https://orcid.org/0000-0002-1274-3237

ESR: https://orcid.org/0000-0001-6234-1300

SGAF: https://orcid.org/0000-0001-6526-3037

KFR: https://orcid.org/0000-0002-0943-2577

SN: https://orcid.org/0000-0003-4692-4543

Abstract

Paleoclimatic variations have profoundly influenced the global distribution of ecosystems and habitats, altering their altitude, spatial configuration, area, and connectivity. Notable examples include island archipelagos and alpine biomes, where shifts in sea-levels and forest lines respectively reshaped their spatial structures. To understand how such changes affected species distributions and biodiversity patterns, we require spatially-explicit reconstructions over continuous time series. However, a comprehensive and reproducible methodology that captures their spatio-temporal dynamism is lacking. Here, we introduce the R package Temporal Altitudinal Biogeographic Shifts (TABS), a tool designed for reconstructing spatial configurations over time, focusing on biogeographic systems bounded by an altitudinal range. We demonstrate the use of TABS by modelling spatial configurations (‘shapes’) of island archipelagos and alpine biomes in response to modulations in sea-levels and forest lines. Unique to TABS, it can also account for crustal deformation due to ice sheet loading and gravitational forces, and for geotectonic and geophysical topographic changes. Beyond past reconstructions, TABS can project spatial configurations shaped by future climatic conditions. This versatile package is easily adaptable to various altitude-bounded biogeographic systems influenced by long-term climatic variations, such as coral reefs and sea shelves. Studying the shifts in biogeographic systems through continuous spatial reconstructions, rather than snapshots in time such as the Last Glacial Maximum, captures the nuances of continuously changing environments and provides a more complete understanding of the biogeography of our planet.

Highlights

- TABS R package enables detailed spatio-temporal reconstructions of biogeographic systems along altitudinal gradients.
- Designed with user-friendliness in mind, it offers a streamlined setup, enabling researchers to start reconstructions quickly without extensive technical expertise.
- TABS is applicable to diverse biogeographic systems, including islands, coastal zones, and mountains.
- It provides flexibility to tailor input data, parameters, and settings according to specific local conditions and research objectives.
- TABS generates outputs using a standardised data structure and open data formats, enabling effective analysis and presentation of results.

Keywords

Quaternary climate change, sea-level fluctuations, spatio-temporal analysis, habitat modelling, paleogeographical reconstructions, climate-driven ecosystem shifts

1 | Introduction

Quaternary climate variations have been a significant driver of evolutionary and ecological processes, profoundly influencing the spatial distribution of biogeographic systems, including habitats, ecosystems and their species communities (Hewitt 2000, Rangel et al. 2018). Climatic variations have repeatedly altered coastlines through sea-level changes, leading to changes in the area and connectivity of terrestrial and marine habitats (Fernández-Palacios et al. 2016, Kealy et al. 2017, 2018). These fluctuations have not only transformed land-sea boundaries (Ali and Aitchison 2014, Weigelt et al. 2016, Norder et al. 2019) but also reshaped the distribution of habitats and species across various ecosystems, from coastal zones to mountainous regions (Sandel et al. 2011, Svenning et al. 2015, Flantua et al. 2019). In particular, altitude-driven biogeographic shifts in mountainous areas, where species respond to warming by moving upslope and to cooling by moving downslope, highlight the dynamic relationship between climate and ecosystem distributions (Rull and Nogué 2007, Dirnböck et al. 2011, Flantua et al. 2014, Flantua and Hooghiemstra 2018). Understanding these historical shifts is crucial for anticipating how future climate changes will continue to reshape the biosphere (Williams et al. 2007), including the distribution of human populations (Wetzel et al. 2012).

Spatio-temporal reconstructions of biogeographic systems are essential for understanding the complex responses of ecosystems to Quaternary climate fluctuations. By quantifying past habitat extent, configuration, and connectivity, these reconstructions provide critical insights into past species distributions. For instance, they allow the identification of key areas, such as refugia and migration routes (Comes and Kadereit 1998) and to find evidence for hypotheses on dispersal among islands in archipelagos (Ali and Aitchison 2014, Rijsdijk et al. 2014a). Especially spatio-temporal reconstructions that analyse changes across longer, continuous time scales provide a more nuanced understanding of biogeographic dynamics than analyses focused on a snapshot in time (Flantua et al. 2019, 2020, Norder et al. 2019). By examining how habitats shifted their distributions across various temporal intervals, we can reveal complex biogeographic patterns of expansion and contraction, and isolation and connectivity, that are otherwise not evident when focusing on isolated time points. Such long-term reconstructions can assess the cumulative effects of climatic fluctuations on islands, such as the effect of changing gene flow (Papadopoulou and Knowles 2015, 2017) and island endemism over time (Ali and Aitchison 2014, Rijsdijk et al. 2014b, Fernández-Palacios et al. 2016). In addition, spatio-temporal connectivity can be quantified to test how changes in habitat (size and suitability) and configuration changed over time (Martensen et al. 2017, Flantua et al. 2019, Huang et al. 2020). This broader temporal perspective of the dynamics of terrestrial and marine habitats worldwide is essential to enable a deeper understanding of how past environments influenced present-day biodiversity, and to provide better predictions of the effect of habitat isolation and connectivity in response to future climate change (McGuire et al. 2016).

Despite the broad interest in spatio-temporal reconstructions, important limitations remain. A key limitation is the absence of a widely accepted, standardised workflow for reconstructing spatio-temporal biogeographic shifts across different systems. Workflows that can seamlessly integrate data from paleoclimatology, geology, ecology, and biogeography are currently absent. Especially the integration of tectonic and isostatic processes is of vital importance for accurate reconstructions in island systems (Whittaker et al. 2017). In addition, numerous studies often rely on discrete temporal snapshots, which fail to capture continuous transitions and cumulative effects critical to understanding long-term biogeographic patterns (Flantua et al. 2020). Also, many workflows may not be easily adaptable across different systems, scales, or temporal resolutions, restricting their application for interdisciplinary adaptability and a broader research community, along with extensive data preparation and technical expertise. Moreover, there is a lack of tools that simultaneously reconstruct past shifts and project future changes under various climate scenarios. Finally, current workflows often fail to provide outputs in open, compatible formats that facilitate further analysis and interdisciplinary collaboration. To address these gaps and advance our understanding of biogeographic dynamics across both space and time, the development of a versatile, user-friendly workflow is essential.

Here, we introduce a globally applicable, reproducible workflow for reconstructing biogeographic shifts in terrestrial and marine environments in response to climate, topography, and geological changes. The Temporal Altitudinal Biogeographic Shifts (TABS) R package models spatial configurations over time, focusing on biogeographic systems bounded by an altitudinal range. Additionally, TABS integrates corrections for crustal deformations and gravitational forces using advanced geophysical models, as opposed to earlier models that often neglected geological dynamics and local context (Rijsdijk et al. 2014b, Norder et al. 2018, Tan et al. 2023). It also allows for adjustments based on local geological conditions, including uplift and subsidence. Furthermore, we expanded its application to mountain systems, building on previous work (Flantua et al. 2019, 2020). TABS is highly versatile, enabling easy modification of input data and parameters to suit local conditions. It produces rapid, accurate reconstructions with minimal manual input, facilitating the modelling and quantification of habitat changes across time. TABS generates outputs that are analytically robust and well-suited for further analysis and publication.

2 |Methods: TABS workflow

2.1 | Functionality

The functionality of TABS (Temporal Altitudinal Biogeographic Shifts) builds on and automates the foundational work laid out by Norder et al. (2018), who developed an R-based workflow to produce a global island and archipelago configuration database. The study combined a global eustatic sea-level curve with a topographic-bathymetric model to reconstruct island area change and configurations, including labelling of individual present and past island polygons. While the workflow from Norder et al. (2018) required manual re-runs to incorporate new datasets, TABS introduces a dynamic, customisable framework. It allows iterative reconstructions that can be fine-tuned based on varying climate and geological conditions and flexible automated label definitions, representing a major leap forward in modelling environmental dynamics. TABS further builds on early work, including the detailed spatio-temporal reconstruction model developed by Simaiakis et al. (2017) further improved by (Rijsdijk et al. 2025) for the Ionian and Aegean sea extents. Both models track island dynamics over the past 26,000 years, but different from Norder et al. (2018) these studies account for local variations in sea-level changes. The latter study also accounts for geological changes to account for the region's tectonic activity. The integration of such complex reconstruction efforts in TABS demonstrated the capacity to model highly complex biogeographic systems with high temporal and spatial resolution. TABS has further expanded to encompass other biogeographic systems, such as high altitude mountain ecosystems, where altitudinal shifts due to temperature changes during the Quaternary period mirror sea-level driven island dynamics (Flantua et al. 2019, 2020). The R package also supports applications for marine biogeographic systems, like the reconstruction of coral reef and shelf sea distributions since the Last Glacial Maximum (De Groeve et al. 2022a). Using a comprehensive set of global datasets and parameter settings, TABS enables the creation of spatial-explicit models representing biogeographic systems worldwide. The next paragraphs describe main datasets and function parameters used by the core function of TABS: *`reconstruct`*.

2.2 | Global Datasets

TABS allows for generating reconstructions using region-specific custom data sources, but various built-in datasets can be used to create reconstructions anywhere on the globe. To enable these datasets, first-time users are encouraged to run the *`setup`* function, which creates a directory structure in a specified or default local path, and automatically downloads these datasets (requiring 15 GB of disk space). Datasets include: i) a tiled version of the global bathymetry and topography (GEBCO Bathymetric Compilation 2024), ii) a spatio-temporal sea-level curve, iii) labelling datasets, including the Global Shoreline Vector (GSV, Sayre et al. 2019), bioclimatic and physical characterisation of the worlds' islands (Weigelt et al. 2013a, 2013b), tectonic plates and orogens (Bird 2003), an open source labelling points dataset for many types of features (GeoNames 2023) and the Global Mountain Biodiversity Assessment (GMBA) Mountain Inventory v2 (Snethlage et al. 2022). These datasets are made available via

Figshare to facilitate and manage any future changes (De Groeve et al. 2022b, 2023, 2024). For instance, the GEBCO model is updated on an annual basis and we aim to upload and announce the integration of most recent versions with upcoming TABS version releases. For more details on dataset sources and examples see vignettes at the TABS website.

2.3 | *Reconstruct* function

The *reconstruct* function is the core function of the TABS R-package and operates with several integrated helper or utility functions (**Fig. 1**). The purpose of this function is to reconstruct and label past or future changes in terrestrial or marine biogeographic systems for a specific region in response to changes in climate and geology. These reconstructions are generated by intersecting a bathymetric or topographic model with a (spatio-temporal) curve and optionally correcting it for regional topographic changes. The resulting reconstructed spatial configurations (hereafter "shapes") of the biogeographic system of interest are optionally named using a labelling dataset. The *reconstruct* function has six main input parameters (*region, reclabs, topo, curve, iso, correction*) and several additional parameters (*buffer, noise(rm), aggregate, fact, units, fillholes, metrics*) that can further fine-tune reconstructions in accordance with the users' needs.

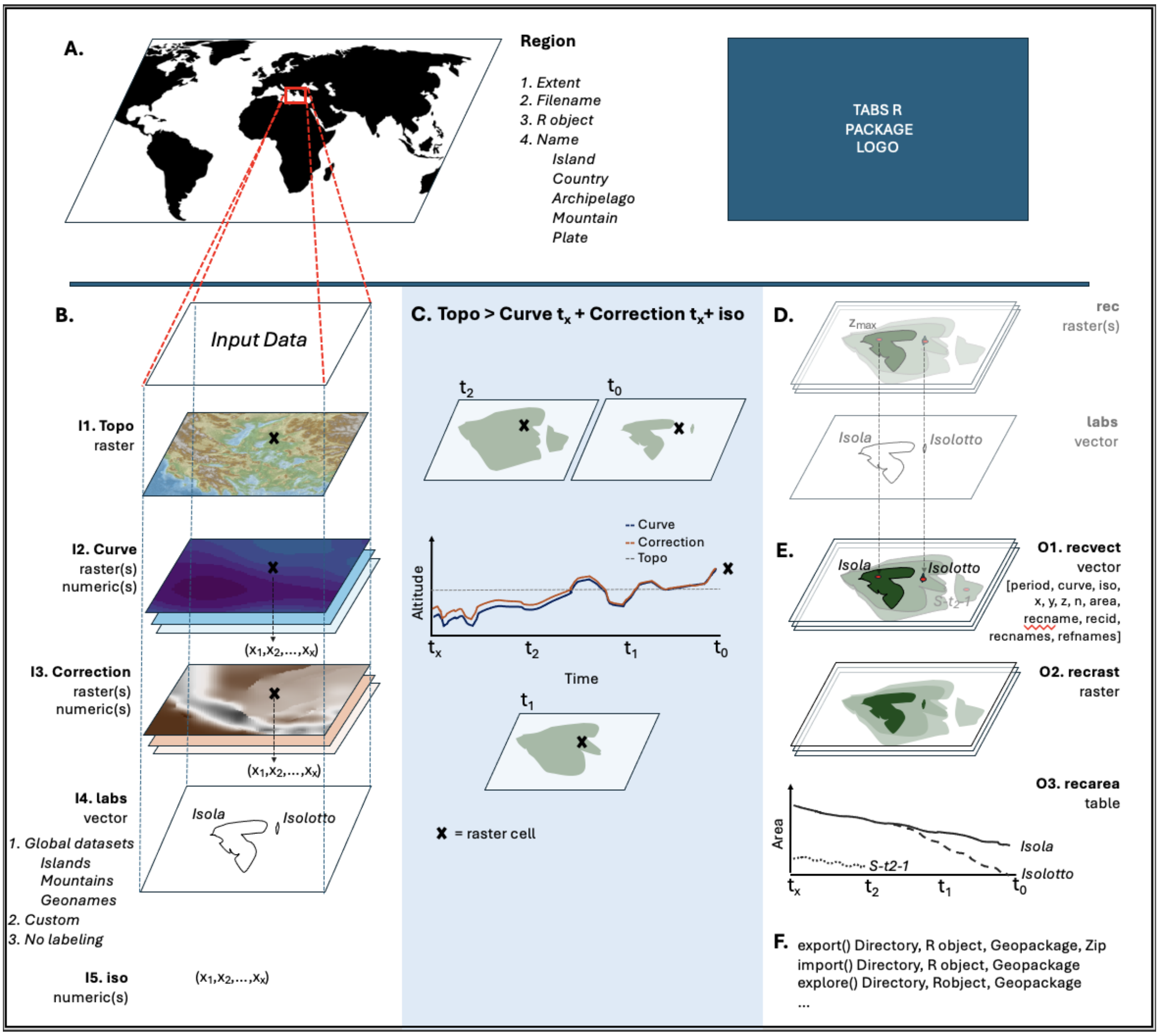

Fig. 1. The infographic provides a summary of the TABS R package and the steps incapsulated by the function *reconstruct*. (A) A region of interest on the globe can be selected using a wide range of methods, including by extent, filename, R objects (e.g., qs_2), or geographic names such as islands, countries, archipelagos, mountains, and tectonic plates. **(B)** For the selected region, a harmonized input data brick is prepared, which includes topography (*topo*, I1), *curve* (I2), *correction* (I3), labels (*labs*, I4), and the altitudinal offset (*iso*, I5). Each dataset can be customized, and both *curve* and *correction* support various formats, including numeric vectors or raster(s). The latter two datasets are intersected with the region of interest and resampled to the resolution of the topography. If needed, the correction dataset is also aligned to the temporal resolution of the curve. The *labs* dataset can be one of the default global datasets (e.g., islands, mountains, geonames), a custom column name, or labelling can be ignored altogether. The *iso* variable defines the altitudinal offset from the curve for a biogeographic system (e.g., corals between 0–30 m BSL), and in this example, it is set to 0. **(C)** Reconstructed shapes are calculated as topographic pixels higher than the sum of the *curve* and *correction*. A line graph illustrates the interaction between these three variables (*topo, curve, correction*) for a single pixel (cross-marked), showing reconstructed shapes for three timestamps (t_0, t_1, t_2). At t_0, the pixel remains below the combined curve-correction threshold, but exceeds it at t_1 and t_2, resulting in reconstructed shapes. **(D/E)** The

generated shapes are then labelled by identifying the highest point in the reconstructed shapes and intersecting them with the labelling dataset. Emerging shapes (e.g., at timestamp t_2) are named using a standard convention (e.g., ‘S’ for shape, time of disappearance, and an identifier). Each shape is also assigned spatial attributes, such as the period, curve and iso, the area (in m^2 and raster cells), x, y, z coordinates, a list of intersecting present-day labels from the labs dataset, and a record of all reconstructed shapes intersecting with the shape at timestamp t_x. **(E)** The *reconstruct* function results in three output datasets: reconstructed shapes in vector and raster formats (recvect, recrast), and reconstructed area estimates for each shape (recarea). **(F)** The final dataset collection includes all the necessary datasets to reproduce the workflow, including all in-and outputs. The dataset collection can be exported, imported, and explored visually using various open data formats, including a (zipped) directory, R object, and geopackage.

`Region` parameter:

To generate a TABS reconstruction, it is important to first define and select the region of interest, which can be done using one of five approaches (**Table 1**): (i) interactive drawing of an extent, (ii) extent coordinates, (iii) path to a local spatial dataset, (iiii) a sf or spatVector R-object, and (iiiii) region-name definitions including islands, archipelagos, countries, tectonic plates and mountains. In total 32,255 region name-definitions are implemented in TABS that can be explored using the built-in *regions* dataset. See more details on region selection on the TABS website’s vignettes.

Table 1. Values and descriptions for the *Region* argument

Description	Value
Default; Interactive drawing of an extent or polygon within R session	`region=NULL`
Specifying the extent as vector or ext-object	`region=c(xmin,xmax,ymin,ymax)`
A path to a locally stored spatial dataset (e.g. shapefile, geopackage)	`region=’filename’`
A spatial (sf, SpatVector) object containing points or shapes	`region='spatvector'`
A name of an island, archipelago, country, tectonic plate or mountain	`region='Greece'` `region='Sporades'`

reclabs parameter:

TABS facilitates labelling of the biogeographic shapes, i.e. naming of each reconstructed shape. To assign such labels, the user can specify the *reclabs* parameter, which includes three approaches (**table 2**). Specifically, (i) labelling using the islands, mountains or geonames global datasets (see 2.2. global datasets), (ii) custom labelling and (iii) automated labelling. With the parameter *aggregate* (boolean; TRUE/FALSE) the spatial scale at which to perform labelling can be defined, specifically for the whole region or for individual reconstructed shapes. For more information on the automatic assigning of labels, see the TABS website’s vignettes.

Table 2. Values and descriptions for *Reclabs* argument

Description	**Value**

labelling using the islands, mountains or geonames global datasets	`reclabs=‘isls’`
	`reclabs=‘mnts’`
	`reclabs=‘peak’`

Custom labelling by specifying the column name of a user-defined region-object	`reclabs=‘name’`
Automatically generated labels	`reclabs=FALSE`
Default; No labelling dataset defined; Labelling depends on the input of the region-object	`reclabs=NULL`

Topo parameter:

By default, the GEBCO grid (2024) is used as the topographic (*topo*) object and consists of both bathymetry and topography at a global scale at a resolution of 30 arcseconds. Alternatively, the user can specify a regional digital elevation model as a path (e.g., `topo=’path_to_file.tif’`). TABS automatically extracts the highest point identified in the topographic object, which is used for labelling reconstructed shapes. The spatial resolution of the *topo* object will be assigned to the TABS outputs (as produced by the *reconstruct* function), unless the resolution factor (*fact*) is modified. Outputs are assigned the projection system of the input *topo* object.

Curve parameter:

The spatio-temporal curve can be defined as any dataset which expresses the relative shift in altitude over time for the biogeographic system of interest. Curves can vary both in space and in time within a region, thus it can be a vector of one or more altitude values, or one or more rasters. A typical example of a curve is a sea-level curve, expressing the change in sea-level compared to the present-day reference (i.e. 0 m RSL). Another example is the upper forest line (UFL), expressing the maximum altitude above present day sea-level at which continuous forest habitat persists. A curve can also be defined by a single value, for instance, the median sea-level across the Pleistocene or a future scenario of sea-level rise. Hence, TABS allows a flexible and customisable definition of a curve. TABS has several built-in curves that can be called by their name (**Table 3**). These curves represent different global sea-level curves (past and future), and an example of a UFL curve for the Northern Andes (*funza*; Torres et al. 2005, Flantua et al. 2019). Note that the shift in altitude should use the same unit as the *topo* object, which is usually expressed in meters. For more details, see the TABS website's vignettes.

277 **Table 3. Spatial-temporal curves**

Name	Description	Time span	Temporal resolution (time steps)	Spatial resolution	Source
Lambeck `curve='Lambeck'`	Global eustatic sea-level curve	35 kyr BP	1000 yr	NA	Lambeck et al. 2014
Cutler `curve='Cutler'`	Global eustatic sea-level curve	120 kyr BP	1000 yr	NA	Cutler et al. 2003
Bintanja `curve='Bintanja'`	Global eustatic sea-level curve	3 Myr BP	1000 yr	NA	(Bintanja and van de Wal 2008)
De Groeve `curve='st_curve'`	Global spatio-temporal sea-level curve	26 kyr BP	500 yr	0.2°	(De Groeve et al. 2022a)
IPCC `curve='SSP1'`	The global average sea-level for four IPCC scenarios (SSP1, SSP2, SSP3, SSP5).	Present day to 2100	20 yr (near, medium, long term)	NA	Intergovernmental Panel on Climate Change (IPCC) 2023
Funza `curve='Funza'`	Upper forest line altitudes derived from fossil pollen record Funza (Colombia)	1 Myr BP – 22 kyr BP	29-1000 kyr	NA	Torres et al. 2005, Flantua et al. 2019
User-defined	A vector with the altitude(s) or a data frame containing altitudes at different time steps.	Any	Any	Any	NA
NULL	If no argument is provided, construction will be produced for the present				

278

279

Iso parameter:

The `iso`(hypse) argument defines the offset from the curve and covers the altitudinal range of the biogeographic system to reconstruct. By default, this argument is set to 0 meter to reconstruct configurations of coastlines and forest lines, but any altitudinal range that describes the altitudinal distribution of a biogeographic region can be used. For example, the availability of corals and shelf seas vary synchronously with sea-level change, thus to reconstruct their spatial configurations we need to specify the minimum and maximum altitude range at which they may occur, respectively 0-30 m BSL and 0-140 m BSL.

Correction parameter:

The reconstruction of biogeographic systems and their spatial configurations over time is influenced not only by specific climatic conditions but also by geotectonic and geophysical activities that result in topographic changes during the study period. For instance, whether an island is above or below the sea-level will not only depend on the redistribution of water from ice sheets, but also local effects that change the topography: such as uplift and subsidence in tectonic active areas, deposition and erosion of sediment in fluvial deltas and land-loss due to catastrophes such as volcanic eruptions. To account for these types of local topographic changes, a `correction` parameter can be defined accounting for (1) temporal linear topographic changes expressed as a rate over time (e.g. mm/yr) and (2) temporal varying topographic changes. Temporal linear topographic changes are expressed in TABS as a single value or raster. Temporally varying topographic changes are expressed as a vector of values, or a list of rasters. Although a database with global correction rates or values does not yet exist, user-defined corrections can be provided for specific regions. As an example, TABS has one built-in regional correction dataset for uplift and subsidence rates in the Sporades, Greece (Rijsdijk et al. 2025). For more details, see the TABS website's vignettes.

Other parameters

In addition to these six main input parameters of *reconstruct*, there are other settings that can be tailored to specific purposes (**Table 1**). A `buffer` can be defined to increase the extent of the `region` definition. With `fillholes`, remaining holes in reconstructed shapes are removed. Further it is possible to identify and remove reconstructed shapes below a specific size (with the `noise` and `noiserm` parameters respectively) and to generate outputs at lower spatial resolution (`fact`). Both `noise(rm)` and `fact` will reduce computation time, since the former will decrease the number of spatial features, and the latter reduces the number of output cells in rasters. The `metrics` parameter specifies which metrics are by default computed, currently only including the area change over time. Moreover, several steps of the `reconstruct` function can be run separately using specific helper-functions, including `get_region`, `get_curve` and `get_correction`.

2.4 | TABS outputs

The two main outputs of the *reconstruct* function are 1) the reconstructed biogeographic shapes at each time step in raster (*recrast*) and vector (*recvect*) format, and 2) a table with the area for each reconstructed shape (*recarea*) per time step and a unique ID assigned to each shape. These IDs allow for tracking which present-day shapes were merged into larger shapes at different time steps. In addition, all preprocessed input datasets are also provided for the defined region (i.e., *topo*, *labs*, *curve*, *correction*). The reconstruct output can be exported in four file formats: (1) directory, where rasters are exported as GEOTIFF and vectors in GeoPackage, (2) zip, a zipped version of directory-type export, (3) rds/qs2, as the default R export data format and (4) gpkg, a full integration of all outputs in a GeoPackage. Outputs can be exported by specifying the argument *`filename`*, including the path and optional extension in the *`reconstruct`* function or in the *`export`* function. Also an *`import`* function is available which allows to load the directory, rds/qs2 or GeoPackage as an R object of class *`tabs`*.

In addition to these in- and outputs that are stored locally, an R object of class *`tabs`* will be generated that can be used to explore the outputs interactively with the *`explore`* function. This function will generate interactive maps to visually explore biogeographic shapes over time, or to compare reconstructed shapes to their present-day distribution.

3. Results: examples of use cases

3.1 | Case study 1: Coastlines - Sporades (Greece)

As a first case study, we reconstructed the coastlines of the Sporades in Greece since the LGM (26 kyr BP) to the present-day using the default input datasets (*topo, labs, curve*). In addition, we defined a correction grid to account for local changes in uplift and subsidence (sample dataset in TABS). Such a complex reconstruction can be run simply by defining four parameters: (1) *region*, as the extent of the correction, (2) *reclabs,* to specify the labeling dataset, (3) *correction*, to account for topographic changes over the last 26 kyr BP and (4) *curve*, set to the spatio-temporal sea-level curve by De Groeve et al. (2022; **Table 2**). Note that inputs *topo* and *labs* are also available as built-in datasets for the extent of the Sporades, but if the default datasets have been downloaded using `setup` it is not necessary to specify the arguments.

```
# load built-in correction grid
correction <- sporades()$correction

# reconstruct
sporades <- reconstruct(region=ext(correction),
                         reclabs="isls", # island labeling dataset
                       correction = correction,
                       curve='st_curve') # call De Groeve curve
```

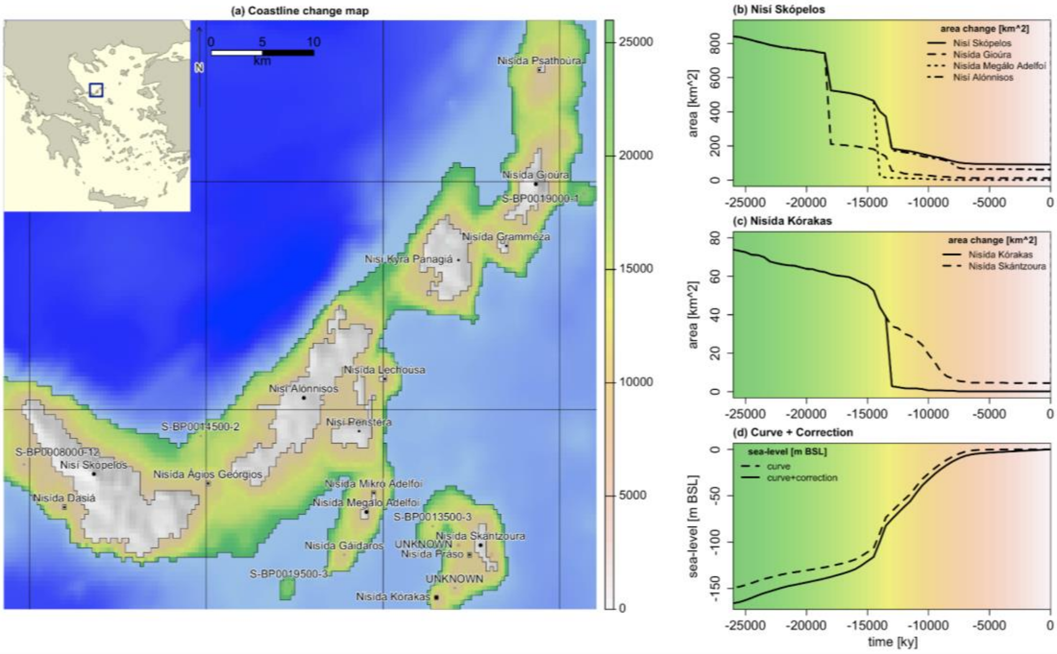

Fig. 2. TABS Reconstruction using the built-in dataset of the Sporades islands (Greece). (a) Coastline change map. Nisi Skopelos (b) and Nisida Kórakas (c) as “macro-islands” tracked

through time. Lines indicate the island areas (y-axis, km^2) at different moments in time (x-axis, yr BP). Separating lines indicate different islands as connections are lost due to changing sea-levels. (d) Sea-level fluctuations at different moments in time (x-axis, yr BP) with and without topographic corrections.

Using the `reconstruct` outputs of TABS, we can create, for example, coastline change maps or graphs representing area change and island connectivity since the LGM due to sea-level fluctuations (Fig. 2). Two island groups remained disconnected from each other (Fig. 2a), here labelled after the highest island of each group, namely Skopelos (Fig. 2b) and Korakas (Fig. 2c). Graphs show that most islands within the Sporades archipelago were connected between 25-18 kyr BP. More specifically, 13 of the 18 present-day islands were interconnected 24 kyr ago, forming the Skopelos island group, while the other 5 present-day islands formed the Korakas island group 14 kyr ago. In addition, five paleo-islands (non-existing islands in present) emerged within the Sporades, of which three merged with the Skopelos island group (S-BP0014500-2, S-BP0008000-12, S-BP0019000-1), one with the Korakas island group (S-BP0013500-3) and one emerged as a separate island 19.5 kyr ago (S-BP0019500-3).

3.2 | Case study 2: Mountains – Andes, Venezuela

In our second case study, we reconstruct the area change of the ‘páramos’ UFL, i.e. high altitude mountain ecosystem in Venezuela (Northern Andes), during the last 1 million years following Flantua et al. (2019). The authors used the reconstructed altitudes of the UFL, based on the long fossil pollen record Funza (Torres et al. 2005), to delimit the lower boundary of the páramos through time. For the implementation of TABS, we used `reconstruct` without labelling and correction grid, while using the default *topo*. Instead of using the entire curve, we calculated decile statistics, representing the proportion of time that the Funza UFL is higher than the given threshold using proportion steps of 0.1. For example, for a proportion of 0.1, the altitude will be above a given UFL-value for 10% of the time (approx. 100 kyr). For these 10 decile-curve values, we ran the *`reconstruct`* function that provided the data outputs necessary to generate the decile map, the curve, and area change in relation to the forest line deciles (Fig. 3 a,b,c). In addition, we also ran the *`reconstruct`* function from 130-29 kyr BP to map the area change over the latter period (Fig. 3 d).

```
# define region using extent coordinates
region <- terra::ext(c(-72.5,-69.2,7.5,10.2))
# curve
curve <- funza[2:length(funza)]
# calculate forest line deciles from curve
deciles <- quantile(curve, probs = seq(0, 1, by = 0.1))

# reconstruct forest line deciles
andes <- reconstruct(region=region,
                     curve=deciles,
                     reclabs=FALSE,
                     aggregate=TRUE)
# reconstruct 0-130 kyr BP
andes130 <- reconstruct(region=region,
                        curve=funza[1:(130-27)],
```

```
                              reclabs=FALSE,
                              aggregate=TRUE)
```

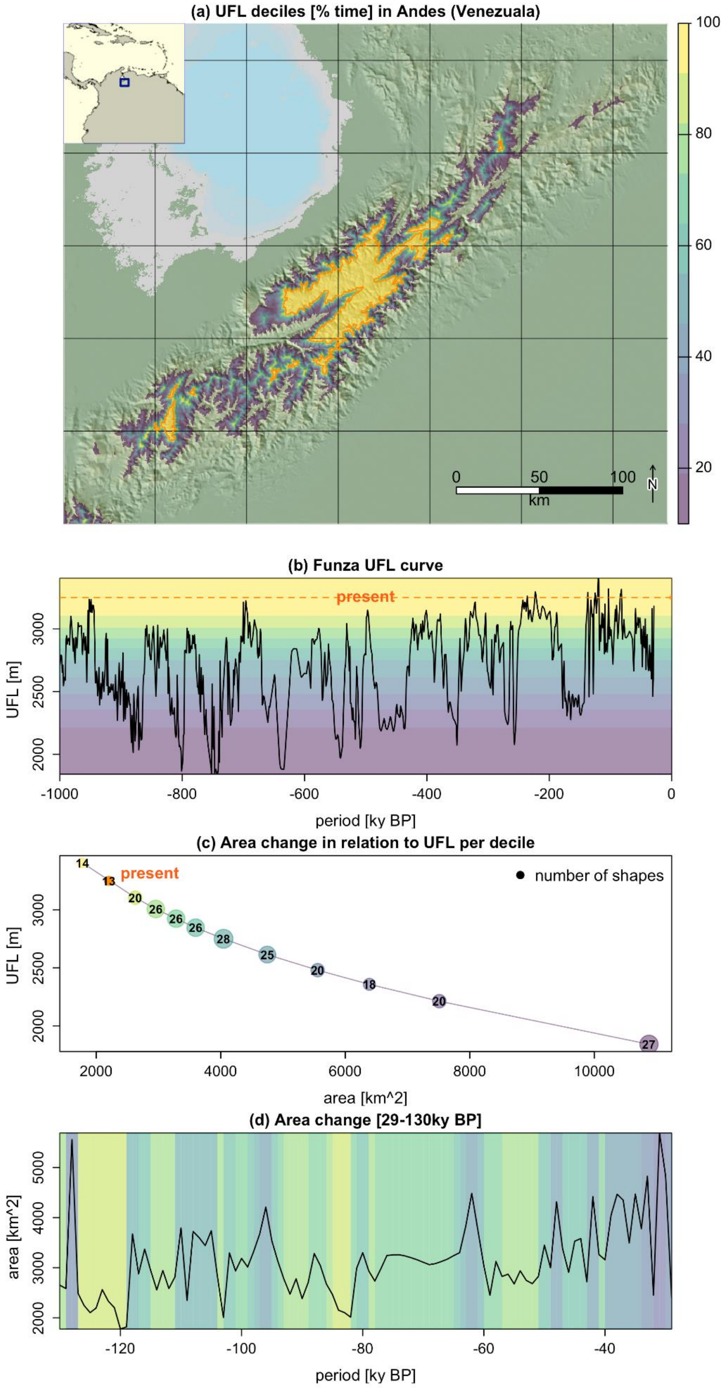

Fig. 3. Reconstructing upper forest line (UFL) deciles, representing the proportion of time during the last 1 million years that the UFL was above an altitudinal threshold. (a) The map

represents the proportion of time (1000-29 kyr BP) that a pixel was above the UFL threshold. (b) Graph shows the altitudinal variation of the Funza UFL from 1000-19 kyr ago with the colored deciles on the background showing the UFL altitudinal range of each decile. (c) Area change in relation to UFL deciles, where the dots show the number of individual “páramo sky islands” at each decile. (d) Area change curve for the last 29-130 kyr BP.

We can see that the present upper forest line (here standardized to UFL = 3250 mASL) is within the upper decile (UFL > 3105 mASL; 2627 km^2), resulting in one of the smallest areal extensions (i.e. 2203 km^2) of the Páramo in comparison to the last 1 million years. More precisely, only for about 13 kyr, or 1.3 % of the time, the UFL was higher and the corresponding area smaller than the present. Half of the time (500 kyr; middle decile) the UFL was below 2750 mASL resulting in the Páramo to be 1.84 times (> 4044 km^2) larger than the present. For 10% of the time (100 kyr; lower decile), the UFL was as low as 2213 mASL, resulting in an areal extension that is about 3.4 times (>7510 km^2) larger than the present (2230 km^2 for a UFL of 3250 mASL).

Discussion and future directions

Here we present TABS as a workhorse for modelling and quantifying spatio-temporal dynamics of biogeographic systems in response to climate and geology. It is built in such a way that it can be used for any biogeographic system that can be roughly defined by an altitudinal range. Specifically, we modelled shorelines of the Sporades archipelago (Greece) and the upper forest lines delimiting the lower boundary of the ‘Páramos’ (high altitude mountain ecosystem of the Northern Andes) as case studies to showcase TABS’ functionality. These case studies illustrate that TABS requires very limited lines of code and a limited number of parameter settings to reconstruct biogeographic shapes over time. While it is easy to generate such reconstructions using default settings, we showcased that TABS is also highly flexible and can incorporate diverse curve representations including RSL rasters in the first use case and (aggregated) UFL vectors in the second. Thanks to TABS' interoperable and standardised output structure, results can be turned into insightful visualisations to investigate patterns of changing biogeographic systems over time. For example, the first use case illustrates the ease of performing automated labelling procedures for both present-day and submerged islands, and how these outputs can be transformed into maps and graphs to analyze past dynamics of island connections. The second use case illustrates how curve (UFL) statistics (i.e. deciles) formalizing boundaries of a biogeographic system can be turned into insightful maps and graphs, representing surface area trends of a system experiencing contraction over time. In short, we illustrated TABS potential to facilitate and enrich scientific analyses with strong visualisations supporting a broad range of biogeographic studies.

Some existing software tools, especially used in the field of island biogeography, are complementary to TABS. The *PleistoDist* R-package (Tan et al. 2023) focuses on visualising and quantifying the effects of eustatic sea-level changes on islands throughout the Pleistocene, providing tools for generating maps and calculating geomorphological metrics. To reconstruct past island areas, *Pleistodist* relies on a global eustatic sea-level curve but does not account for other types of topographic changes due to geological and geomorphological processes (Tan et al., 2023). In contrast, TABS has a suite of built-in curves, including a spatio-temporal curve that accounts for local sea-level variations (De Groeve et al. 2022a). Furthermore, new and improved spatio-temporal sea-level models, or other curves (e.g. UFL curves), can be easily integrated in TABS. The R-package *DAISIE* (Valente et al. 2015) models island biota change dynamically through speciation, immigration, and extinction, using phylogenetic trees to estimate colonisation, speciation, and extinction rates. In the future, we aim to link or integrate TABS with complementary tools like *`PleistoDist`* and *`DAISIE`*, enabling the use of TABS outputs to improve predictions of colonization, speciation, and extinction rates, as well as calculations of geomorphological metrics.

The performance of TABS is dependent on the complexity of the reconstruction. For instance, generating reconstructions using GEBCO and an eustatic curve, which has been the practice in literature until now (Norder et al. 2018, Tan et al. 2023), will be significantly faster than a reconstruction using high-resolution, local topographic models and spatio-temporal curves. Accounting for local variations by defining a correction grid will further decrease the speed of calculations but will result in more accurate reconstructions. Hence there is a tradeoff between performance and accuracy of the reconstruction and its derived metrics such as area change. The resolution of the input topographic dataset will largely define the quality of the labelling and recognition of shapes. The higher the resolution of the *`topo`* `dataset`, the more likely that labelling is done correctly, and the more likely that shapes are identified as separate units. For instance, islands separated by narrow sea streets, like Sicily from mainland Italy and Evia from mainland Greece, will not be distinguished as separate shapes and be included in the continent if no accurate topographic model is available. Also, small shapes, such as islets, will be much better identified using accurate topographic models.

Improvements and future developments TABS

Global vs regional reconstructions: Currently, TABS is customised for regional reconstructions across the globe and not for continuous global reconstructions, such as the global shoreline and shelf sea rasters (De Groeve et al. 2022a). Such global reconstructions are also aimed to be integrated in a future release of TABS. However, TABS can be used for global studies by subsequent definition of extents, for instance a list of archipelagos. Using standard iteration functions (*e.g.* `sapply, lapply`), biogeographic systems can then be reconstructed for each subsequent area of interest.

Naming: Automated labelling of biogeographic shapes is currently only integrated for shoreline objects (continents, islands, islets) and mountain ranges. The default labelling option is based on GSV (Sayre et al. 2019) for shoreline shapes, or GMBA (Snethlage et al. 2022) for mountain shapes. Hence, labelling based on other geotags, such as coral bed names, requires the definition of custom labelled points or shapes. When using custom points, it is essential to define locations that have a high probability to fall within the present-day biogeographic shapes (such as highest points or centroids), otherwise, points might not intersect with the reconstructed shapes. Another approach could be to export first a present-day reconstruction, to explore which reconstructed shapes are recognised, edit the shape names, and use this input as the labelling dataset.

Furthermore, labelling of reconstructed shapes is primarily based on the location of the highest point observed within the underlying topography. This is a valid naming convention for biogeographic systems which only have a lower range limit, such as shorelines as well as upper forest lines, but not for biogeographic systems defined by a range, such as corals or shelf seas. This is because the highest point is not constant and shifts horizontally with every sea-level change. A more advanced procedure is required to enable labelling of shapes during horizontal biogeographic shifts. Reconstructions that do not require labelling or only require area change reconstructions at the extent level are applicable for any biogeographic range definition.

Corrections: While corrections can be integrated in the model, either through definition of a (list of) grids or values, it is expected from the user to prepare this input. This is particularly time consuming if corrections are defined as grids requiring potential data collection, integration and manipulation. Given that there are no integrated databases including rates of topographic change (e.g. uplift, subsidence, erosion, sedimentation) a user will need to first screen the literature to collect known rates for locations within the study area. These rates can be digitised as linear features, in case of linear breakpoints, or as point features, in case rates are known for a specific location. Further, it might be necessary to define support points to enhance and facilitate the interpolation to obtain a smoothed grid accounting also for breakpoints. In case rates are not linear, and vary over time, the process will need to be repeated for every period. For more details on the workflow, see Rijsdijk et al. (2025) who present a correction grid for the Aegean Archipelago. In the future, we aim to facilitate this procedure by creating (1) a point and linear feature database with topographic rates of change, (2) an interpolation function, accounting for breakpoint features.

Isolation metrics and visualisations: We aim to further integrate more functionalities to TABS, including other pre-calculated metrics than area change, such as distance between shapes and timing of isolation. We also aim to integrate functions for default publication ready visualisations including maps, connectivity metrics and curve changes for the selected region or reconstructed shapes.

We encourage researchers interested in using TABS to contact our team for potential collaborations, allowing us to better address user-specific needs and further optimize the tool for diverse applications. For reporting bugs and recommendations, we advise to create an issue in the TABS gitlab repository (https://gitlab.com/uva_ibed_piac/tabs/-/issues).

Conclusion

In conclusion, TABS is just as intuitive as pressing the *Tab* key—streamlining the complex process of reconstructing spatio-temporal biogeographic configurations. By effortlessly mapping surface area changes, connectivity, and isolation over time, TABS generates structured geospatial datasets ready-to-use for further analysis and visualization. Its customizable parameters can be adapted to any local environment, making it a valuable tool for researchers aiming to model and quantify habitat changes over temporal scales, anywhere on the globe.

References

Ali JR, Aitchison JC (2014) Exploring the combined role of eustasy and oceanic island thermal subsidence in shaping biodiversity on the Galápagos. Journal of Biogeography 41: 1227–1241. https://doi.org/10.1111/jbi.12313

Bintanja R, van de Wal RSW (2008) North American ice-sheet dynamics and the onset of 100,000-year glacial cycles. Nature 454: 869–872. https://doi.org/10.1038/nature07158

Bird P (2003) An updated digital model of plate boundaries. Geochemistry, Geophysics, Geosystems 4. https://doi.org/10.1029/2001GC000252

Comes HP, Kadereit JW (1998) The effect of Quaternary climatic changes on plant distribution and evolution. Trends in Plant Science 3: 432–438. https://doi.org/10.1016/S1360-1385(98)01327-2

Cutler KB, Edwards RL, Taylor FW, Cheng H, Adkins J, Gallup CD, Cutler PM, Burr GS, Bloom AL (2003) Rapid sea-level fall and deep-ocean temperature change since the last interglacial period. Earth and Planetary Science Letters 206: 253–271. https://doi.org/10.1016/S0012-821X(02)01107-X

De Groeve J, Norder S, Rijsdijk KF (2024) Tiled version of GEBCO sub ice topo. https://doi.org/10.21942/uva.23943957.v3

De Groeve J, Kusumoto B, Koene E, Kissling WD, Seijmonsbergen AC, Hoeksema BW, Yasuhara M, Norder SJ, Cahyarini SY, van der Geer A, Meijer HJM, Kubota Y, Rijsdijk KF (2022a) Global raster dataset on historical coastline positions and shelf sea extents since the Last Glacial Maximum. Global Ecology and Biogeography 31: 2162–2171. https://doi.org/10.1111/geb.13573

De Groeve J, Kusumoto B, Koene E, Kissling WD, Seijmonsbergen AC, Hoeksema BW, Yasuhara M, Norder SJ, Cahyarini SY, Geer A van der, Meijer HJM, Kubota Y, Rijsdijk KF (2022b) Spatio-Temporal Relative Sea Level Curve (RSL). https://doi.org/10.21942/uva.20029991.v1

De Groeve JD, Norder SJ, Rijsdijk KF, Flantua S, rentier eline (2023) Island, archipelago, plate, mountain and point labeling dataset. https://doi.org/10.21942/uva.22788464.v5

Dirnböck T, Essl F, Rabitsch W (2011) Disproportional risk for habitat loss of high-altitude endemic species under climate change. Global Change Biology 17: 990–996. https://doi.org/10.1111/j.1365-2486.2010.02266.x

Fernández-Palacios JM, Rijsdijk KF, Norder SJ, Otto R, de Nascimento L, Fernández-Lugo S, Tjørve E, Whittaker RJ (2016) Towards a glacial-sensitive model of island biogeography. Global Ecology and Biogeography 25: 817–830. https://doi.org/10.1111/geb.12320

Flantua S, Hooghiemstra H (2018) Historical connectivity and mountain biodiversity. Available from: https://www.semanticscholar.org/paper/Historical-connectivity-and-mountain-biodiversity-Flantua-Hooghiemstra/c7a44200cca79297ca5a0b6ed3c065132bc66615 (December 23, 2024).

Flantua SG, Hooghiemstra H, Van Boxel JH, Cabrera M, González-Carranza Z, González-Arango C (2014) Connectivity dynamics since the Last Glacial Maximum in the northern Andes; a pollen-driven framework to assess potential migration. Paleobotany and Biogeography: A Festschrift for Alan Graham in His 80th Year. Missouri Botanical Garden, St. Louis: 98–123. Available from: https://www.academia.edu/download/41747781/Connectivity_dynamics_since_the_Last_Gla20160129-16042-t953fg.pdf (February 25, 2025).

Flantua SGA, O'Dea A, Onstein RE, Giraldo C, Hooghiemstra H (2019) The flickering connectivity system of the north Andean páramos. Journal of Biogeography 46: 1808–1825. https://doi.org/10.1111/jbi.13607

Flantua SGA, Payne D, Borregaard MK, Beierkuhnlein C, Steinbauer MJ, Dullinger S, Essl F, Irl SDH, Kienle D, Kreft H, Lenzner B, Norder SJ, Rijsdijk KF, Rumpf SB, Weigelt P, Field R (2020) Snapshot isolation and isolation history challenge the analogy between mountains and islands used to understand endemism. Global Ecology and Biogeography 29: 1651–1673. https://doi.org/10.1111/geb.13155

GEBCO Bathymetric Compilation G (2024) GEBCO_2024 Grid. British Oceanographic Data Centre. https://doi.org/10.5285/1c44ce99-0a0d-5f4f-e063-7086abc0ea0f

GeoNames (2023) GeoNames. Available from: https://download.geonames.org/export/dump/ (February 25, 2025).

Hewitt G (2000) The genetic legacy of the Quaternary ice ages. Nature 405: 907–913. https://doi.org/10.1038/35016000

Huang J-L, Andrello M, Martensen AC, Saura S, Liu D-F, He J-H, Fortin M-J (2020) Importance of spatio–temporal connectivity to maintain species experiencing range shifts. Ecography 43: 591–603. https://doi.org/10.1111/ecog.04716

Intergovernmental Panel on Climate Change (IPCC) (Ed.) (2023) Atlas. In: Climate Change 2021 – The Physical Science Basis: Working Group I Contribution to the Sixth Assessment Report of the Intergovernmental Panel on Climate Change. Cambridge University Press, Cambridge, 1927–2058. https://doi.org/10.1017/9781009157896.021

Kealy S, Louys J, O'Connor S (2017) Reconstructing Palaeogeography and Inter-island Visibility in the Wallacean Archipelago During the Likely Period of Sahul Colonization, 65–45 000 Years Ago. Archaeological Prospection 24: 259–272. https://doi.org/10.1002/arp.1570

Kealy S, Louys J, O'Connor S (2018) Least-cost pathway models indicate northern human dispersal from Sunda to Sahul. Journal of Human Evolution 125: 59–70. https://doi.org/10.1016/j.jhevol.2018.10.003

Lambeck K, Rouby H, Purcell A, Sun Y, Sambridge M (2014) Sea level and global ice volumes from the Last Glacial Maximum to the Holocene. Proceedings of the National Academy of Sciences 111: 15296–15303. https://doi.org/10.1073/pnas.1411762111

Martensen AC, Saura S, Fortin M-J (2017) Spatio-temporal connectivity: assessing the amount of reachable habitat in dynamic landscapes. Methods in Ecology and Evolution 8: 1253–1264. https://doi.org/10.1111/2041-210X.12799

McGuire JL, Lawler JJ, McRae BH, Nuñez TA, Theobald DM (2016) Achieving climate connectivity in a fragmented landscape. Proceedings of the National Academy of Sciences 113: 7195–7200. https://doi.org/10.1073/pnas.1602817113

Norder SJ, Baumgartner JB, Borges PAV, Hengl T, Kissling WD, van Loon EE, Rijsdijk KF (2018) A global spatially explicit database of changes in island palaeo-area and archipelago configuration during the late Quaternary. Global Ecology and Biogeography 27: 500–505. https://doi.org/10.1111/geb.12715

Norder SJ, Proios K, Whittaker RJ, Alonso MR, Borges PAV, Borregaard MK, Cowie RH, Florens FBV, de Frias Martins AM, Ibáñez M, Kissling WD, de Nascimento L, Otto R, Parent CE, Rigal F, Warren BH, Fernández-Palacios JM, van Loon EE, Triantis KA, Rijsdijk KF (2019) Beyond the Last Glacial Maximum: Island endemism is best explained by long-lasting archipelago configurations. Global Ecology and Biogeography 28: 184–197. https://doi.org/10.1111/geb.12835

Papadopoulou A, Knowles LL (2015) Genomic tests of the species-pump hypothesis: Recent island connectivity cycles drive population divergence but not speciation in Caribbean crickets across the Virgin Islands. Evolution 69: 1501–1517. https://doi.org/10.1111/evo.12667

Papadopoulou A, Knowles LL (2017) Linking micro- and macroevolutionary perspectives to evaluate the role of Quaternary sea-level oscillations in island diversification. Evolution 71: 2901–2917. https://doi.org/10.1111/evo.13384

Rangel TF, Edwards NR, Holden PB, Diniz-Filho JAF, Gosling WD, Coelho MTP, Cassemiro FAS, Rahbek C, Colwell RK (2018) Modeling the ecology and evolution of biodiversity: Biogeographical cradles, museums, and graves. Science 361: eaar5452. https://doi.org/10.1126/science.aar5452

Rijsdijk KF, Hengl T, Norder SJ, Otto R, Emerson BC, Ávila SP, López H, van Loon EE, Tjørve E, Fernández-Palacios JM (2014a) Quantifying surface-area changes of volcanic islands driven by Pleistocene sea-level cycles: biogeographical implications for the Macaronesian archipelagos. Journal of Biogeography 41: 1242–1254. https://doi.org/10.1111/jbi.12336

Rijsdijk KF, Hengl T, Norder SJ, Otto R, Emerson BC, Ávila SP, López H, van Loon EE, Tjørve E, Fernández-Palacios JM (2014b) Quantifying surface-area changes of volcanic islands driven by Pleistocene sea-level cycles: biogeographical implications for the Macaronesian archipelagos. Journal of Biogeography 41: 1242–1254. https://doi.org/10.1111/jbi.12336

Rull V, Nogué S (2007) Potential migration routes and barriers for vascular plants of the Neotropical Guyana Highlands during the Quaternary. Journal of Biogeography 34: 1327–1341. https://doi.org/10.1111/j.1365-2699.2006.01602.x

Sandel B, Arge L, Dalsgaard B, Davies RG, Gaston KJ, Sutherland WJ, Svenning J-C (2011) The Influence of Late Quaternary Climate-Change Velocity on Species Endemism. Science 334: 660–664. https://doi.org/10.1126/science.1210173

Sayre R, Noble S, Hamann S, Smith R, Wright D, Breyer S, Butler K, Van Graafeiland K, Frye C, Karagulle D, Hopkins D, Stephens D, Kelly K, Basher Z, Burton D, Cress J, Atkins K, Van Sistine DP, Friesen B, Allee R, Allen T, Aniello P, Asaad I, Costello MJ, Goodin K, Harris P, Kavanaugh M, Lillis H, Manca E, Muller-Karger F, Nyberg B, Parsons R, Saarinen J, Steiner J, Reed A (2019) A new 30 meter resolution global shoreline vector and associated global islands database for the development of standardized ecological coastal units. Journal of Operational Oceanography 12: S47–S56. https://doi.org/10.1080/1755876X.2018.1529714

Simaiakis SM, Rijsdijk KF, Koene EFM, Norder SJ, Van Boxel JH, Stocchi P, Hammoud C, Kougioumoutzis K, Georgopoulou E, Van Loon E, Tjørve KMC, Tjørve E (2017) Geographic changes in the Aegean Sea since the Last Glacial Maximum: Postulating biogeographic effects of sea-level rise on islands. Palaeogeography, Palaeoclimatology, Palaeoecology 471: 108–119. https://doi.org/10.1016/j.palaeo.2017.02.002

Snethlage MA, Geschke J, Ranipeta A, Jetz W, Yoccoz NG, Körner C, Spehn EM, Fischer M, Urbach D (2022) A hierarchical inventory of the world’s mountains for global comparative mountain science. Scientific Data 9: 149. https://doi.org/10.1038/s41597-022-01256-y

Svenning J-C, Eiserhardt WL, Normand S, Ordonez A, Sandel B (2015) The Influence of Paleoclimate on Present-Day Patterns in Biodiversity and Ecosystems. Annual Review of Ecology, Evolution, and Systematics 46: 551–572. https://doi.org/10.1146/annurev-ecolsys-112414-054314

Tan DJX, Gyllenhaal EF, Andersen MJ (2023) PleistoDist: A toolbox for visualising and quantifying the effects of Pleistocene sea-level change on island archipelagos. Methods in Ecology and Evolution 14: 496–504. https://doi.org/10.1111/2041-210X.14024

Torres V, Vandenberghe J, Hooghiemstra H (2005) An environmental reconstruction of the sediment infill of the Bogotá basin (Colombia) during the last 3 million years from abiotic and biotic proxies. Palaeogeography, Palaeoclimatology, Palaeoecology 226: 127–148. https://doi.org/10.1016/j.palaeo.2005.05.005

Valente LM, Phillimore AB, Etienne RS (2015) Equilibrium and non-equilibrium dynamics simultaneously operate in the Galápagos islands. Ecology Letters 18: 844–852. https://doi.org/10.1111/ele.12461

Weigelt P, Jetz W, Kreft H (2013a) Bioclimatic and physical characterization of the world’s islands. Proceedings of the National Academy of Sciences 110: 15307–15312. https://doi.org/10.1073/pnas.1306309110

Weigelt P, Jetz W, Kreft H (2013b) Data from: Bioclimatic and physical characterization of the world’s islands. : 7051753 bytes. https://doi.org/10.5061/DRYAD.FV94V

Weigelt P, Steinbauer MJ, Cabral JS, Kreft H (2016) Late Quaternary climate change shapes island biodiversity. Nature 532: 99–102. https://doi.org/10.1038/nature17443

Wetzel FT, Kissling WD, Beissmann H, Penn DJ (2012) Future climate change driven sea-level rise: secondary consequences from human displacement for island biodiversity. Global Change Biology 18: 2707–2719. https://doi.org/10.1111/j.1365-2486.2012.02736.x

Whittaker RJ, Fernández-Palacios JM, Matthews TJ, Borregaard MK, Triantis KA (2017) Island biogeography: Taking the long view of nature’s laboratories. Science 357: eaam8326. https://doi.org/10.1126/science.aam8326

Williams JW, Jackson ST, Kutzbach JE (2007) Projected distributions of novel and disappearing climates by 2100 AD. Proceedings of the National Academy of Sciences 104: 5738–5742. https://doi.org/10.1073/pnas.0606292104

Acknowledgements

ESR and SGAF acknowledge financial support from Trond Mohn Stiftelse (TMS) and the University of Bergen for the startup grant 'TMS2022STG03’ to S.G.A.Flantua. JDG was supported by institutional resources from the Computational Support Team of the Institute for Biodiversity and Ecosystem Dynamics (IBED), University of Amsterdam (Netherlands). We would like to thank scientific illustrator Miranta Kouvari for preparing the graphical abstract and R logo supported by the grant 'TMS2022STG03’ to S.G.A.Flantua and by IBED institutional budgets.

Author contributions statement

JDG: Writing - Original draft, Writing - Review and Editing, Visualisation, Software, Data curation, Methodology, Project Administration, Conceptualisation

SJN: Writing - Original draft, Writing - Review and Editing, Resources, Methodology, Project Administration, Conceptualisation

KFR: Writing - Review and Editing, Project Administration, Methodology, Resources, Conceptualisation

ESR: Writing - Review and Editing, Project Administration, Validation, Conceptualisation

SGAF: Writing - Review and Editing, Project Administration, Resources, Funding Acquisition, Conceptualisation

Data Accessibility Statement

TABS is accessible via https://gitlab.com/uva_ibed_piac/tabs and upon acceptance will be linked to Zenodo with the corresponding DOI and reference. We intend to also submit the package to CRAN. All default global datasets can be accessed at Figshare (De Groeve et al. 2022b, 2023, 2024).